Available online at www.sciencedirect.com
ScienceDirect
Journal of Molecular Catalysis A: Chemical 256 (2006) 324–334
JOURNAL OF MOLECULAR CATALYSIS A: CHEMICAL
www.elsevier.com/locate/molcata

Heteropoly acid supported on titania as solid acid catalyst in alkylation of *p*-cresol with *tert*-butanol

Suresh M. Kumbar [a], G.V. Shanbhag [a], F. Lefebvre [b], S.B. Halligudi [a,*]

[a] *Inorganic Chemistry & Catalysis Division, National Chemical Laboratory, Pune 411 008, India*
[b] *Laboratoire de Chimie Organométallique de Surface, CNRS-CPE, Villeurbanne Cedex, France*

Received 7 April 2006; received in revised form 5 May 2006; accepted 11 May 2006
Available online 13 June 2006

Abstract

Butylation of *p*-cresol with *tert*-butanol was investigated on titania modified with 12-tungstophosphoric acid (TPA/TiO_2) catalyst under vapor phase conditions. Catalysts with different TPA loadings (10–25 wt.%) and calcination temperatures (650–750 °C) were prepared by suspending titanium hydroxide in methanol solution of TPA followed by drying and calcination. These catalysts were characterized by surface area, XRD, ^{31}P MAS NMR, XPS, NH_3-TPD, and FTIR pyridine adsorption. XRD results indicated that the presence of TPA retarded the crystallization of titania and stabilized TiO_2 in anatase phase. ^{31}P MAS NMR indicated the presence of TPA in various forms (dispersed, highly fragmented and Keggin intact). These catalysts showed both Brönsted and Lewis acidity, and 20% TPA on TiO_2 calcined at 700 °C (from here after words 20% TT-700) had the highest Brönsted as well as total acidity. Further, the catalytic activities were examined in *tert*-butylation of *p*-cresol with *tert*-butanol. The catalytic activity depended on TPA coverage, and the highest activity corresponded to the monolayer of TPA on titania. The most active catalyst 20% TT-700 gave 82% conversion of *p*-cresol and 89.5% selectivity towards 2-*tert*-butyl cresol (TBC), 2,6-di-*tert*-butyl cresol (DTBC) 7.5% and cresol-*tert*-butyl ether (CTBE) 3% under optimized conditions. The activity was always higher than that of WO_3/ZrO_2, sulfated zirconia (SZ), USY, H-β zeolites and montmorillonite K-10 (K-10mont) under similar conditions.

Keywords: Heteropoly acid; Titania; *p*-Cresol; *tert*-Butanol; 2-*tert*-Butyl-*p*-cresol; 2,6-Di-*tert*-butyl-*p*-cresol; Alkylation

1. Introduction

Eco-friendly and commercially viable catalyst systems are in demand for selective alkylation and acylation of aromatic substrates to corresponding value added products. Friedel–Crafts catalysts such as $AlCl_3$, $FeCl_3$ and $ZnCl_2$ are still used for alkylation of aromatics. But these catalyst systems are least preferred as alkylating agents since they generate many problems such as pollution, handling, safety, corrosion and tedious work up. As solid acids are non-corrosive and can be handled and separated easily from the liquid reaction mixtures there are the some attempts to replace the above-mentioned Lewis or mineral acids by strong solid acids based on supported transition metal oxides in electrophilic aromatic substitutions [1,2]. Alkylation of *p*-cresol with *tert*-butanol gives 2-*tert*-butyl-*p*-cresol and 2,6-di-*tert*-butyl-*p*-cresol, commercially known as butylated hydroxy toluene (BHT), which are widely used in the manufacture of phenolic resins, as antioxidants [3] and polymerization inhibitors [4]. Alkylation of *p*-cresol with benzyl alcohol using stoichiometric amount of $AlCl_3$ [5] and butylation of *o*-cresol with *tert*-butanol using stoichiometric amount of H_3PO_4 [6] have been reported. In spite of the industrial importance of the butylation of *p*-cresol to get BHT, not much work has been reported in the literature. Solid acid catalysts such as cation exchange resins have been used as catalysts for the above reaction [7,8]. Butylation of *p*-cresol has been carried out with isobutylene as an alkylating agent using sulfated zirconia [9]. Recently, 12-tungstophosphoric acid immobilized on macroporous phenol–furfural sulphonic acid resin using γ-aminopropyltriethoxy silane catalyst has been used for butylation of *p*-cresol [10]. Heteropoly acids supported on solid metal oxides with high surface area, which are thermally stable, have been gaining importance as alkylating and acylating catalysts [11–15]. Supported salts of heteropoly acids can also been effectively used in many alkylation and acylation reactions [16–18] while solid acid catalysts such as TPA/ZrO_2, WO_3/ZrO_2 have

* Corresponding author.
E-mail address: sb.halligudi@ncl.res.in (S.B. Halligudi).

1381-1169/$ – see front matter © 2006 Elsevier B.V. All rights reserved.
doi:10.1016/j.molcata.2006.05.024

been studied for the above reaction [18–21]. Titania, a widely used catalyst support [22], is known to enhance the activity in many cases due to the strong interaction between the active phase and the support [23]. Titania has three crystalline phases: rutile, anatase, and brookite. Rutile is the thermodynamically stable state, whereas the other two phases are metastable [24]. Because the crystalline state and structure of the support strongly affect the catalytic activity and selectivity, the design and selection of novel, highly active catalysts places many requirements on the supports used.

The present study deals with the preparation of titania supported 12-tungstophosphoric acid and its characterization by various analytical and spectroscopic techniques such as surface area, XRD, TPD, ^{31}P MAS NMR, XPS and pyridine FTIR. The catalytic activities of these catalysts were evaluated in alkylation of *p*-cresol with *tert*-butanol. The most active 20% TT-700 (TPA/TiO_2) catalyst was compared with WO_3/ZO_2, sulfated zirconia (SZ), zeolites like USY, H-β and montmorillonite K-10 (K-mont).

2. Experimental

2.1. Materials

12-Tungstophosphoric acid, *p*-cresol and *tert*-butanol were purchased from s.d.fine Chemicals Ltd., Mumbai. Titanium (IV) butoxide was procured from Loba Chemie Ltd., Mumbai. Methanol was purchased from E.Merck India Ltd., Mumbai. TPA ($H_3PW_{12}O_{40}\cdot nH_2O$), montmorillonite K-10 were purchased from Aldrich. Sulfated zirconia was obtained from MEL Chemicals; zeolites USY (Si/Al = 9) and H-β (Si/Al = 40) were provided by the PQ Corporation. All the chemicals were research grade and were used without further purification in the catalyst preparation and butylation experiments.

2.2. Catalyst preparation

The catalysts were prepared by suspending a known amount of dried titanium hydroxide powder in a methanol solution of TPA. Titanium hydroxide was prepared by hydrolysis of titanium (IV) butoxide by drop wise addition of distilled water. The precipitate was filtered and washed with distilled water. The titanium hydroxide thus obtained was dried at 120 °C for 12 h, well powdered, and dried for another 12 h.

For the preparation of TPA supported catalysts the following procedure was used: In each case, 4 ml of TPA solution in methanol per gram of solid support was used, and the mixture was stirred in a rotary evaporator for 8–10 h. The excess of methanol was removed at 50 °C under vacuum. The resulting solid was dried at 120 °C for 24 h and well ground. A series of catalysts with different TPA loadings (10–25%) were prepared by varying the TPA concentration in methanol. The dried samples were finally calcined in air. All samples were calcined in a shallow quartz boat placed inside a 3-cm-diameter quartz tube in a tube furnace. The samples were heated at the rate of 5 °C min^{-1} to the final temperature, held for 4 h under static conditions and then cooled to room temperature at the rate of 5 °C min^{-1}.

2.3. Characterization

The specific surface areas of the catalysts were measured by N_2 physisorption at liquid nitrogen temperature using a QuantachromeNova-1200 surface area analyzer and standard multipoint BET analysis methods. Samples were degassed in flowing N_2 for 2 h at 300 °C before N_2 physisorption measurements.

X-ray diffraction (XRD) measurement of the catalyst powder were recorded using a Rigaku Geigerflex diffractometer equipped with Ni-filtered Cu Kα radiation (λ = 1.5418 Å).

The ^{31}P MAS NMR spectrum of the TPA/TiO_2 catalysts having different TPA loadings calcined at 700 °C were recorded using a Bruker DSX-300 spectrometer at 121.5 MHz with high-power decoupling with a Bruker 4-mm probe head. The spinning rate was 10 kHz, and the delay between two pulses was varied between 1 and 30 s to ensure complete relaxation of the ^{31}P nuclei. The chemical shifts are expressed relative to external 85% H_3PO_4.

X-ray photoelectron spectroscopy (XPS) measurement of the catalysts were performed on a VG Microtech Multilab ESCA 3000 spectrometer with a non-monochromatized Mg Kα X-ray source. Energy resolution of the spectrometer was set at 0.8 eV with Mg Kα radiation at pass energy of 50 eV. The binding energy correction was performed using the C1s peak of carbon at 284.6 eV as a reference.

The total acidity of the catalysts was measured by temperature programmed desorption of NH_3 (NH_3-TPD) using a Micromeritics AutoChem-2910 instrument. It was carried out after ∼0.5 g of the catalyst sample was dehydrated at 600 °C in helium (30 cm^3 min^{-1}) flow for 1 h. The temperature was decreased to 100 °C, and NH_3 was adsorbed by exposing samples treated in this manner to a stream containing 10% NH_3 in helium for 1 h at 100 °C. It was then flushed with helium for another 1 h to remove physisorbed NH_3. The desorption of NH_3 was carried out in helium flow (30 cm^3 min^{-1}) by increasing the temperature to 600 °C at the rate of 10 °C min^{-1} and measuring NH_3 desorption using a TCD detector.

The nature of the acid sites (Brönsted and Lewis) of the catalyst samples was determined by in situ Fourier transform infrared (FTIR) spectroscopy with chemisorbed pyridine. The pyridine adsorption studies were carried out in the diffuse reflectance infrared Fourier transform (DRIFT) mode using a Shimadzu SSU 8000 instrument. A calcined powder sample in a sample holder was placed in a specially designed cell. The samples were then heated in situ under a flow (40 ml min^{-1}) of pure N_2. The samples were kept at 400 °C for 3 h, then cooled to 100 °C; pyridine vapor (20 μl) was then introduced under N_2 flow, and the IR spectra were recorded at different temperatures up to 400 °C. A resolution of 4 cm^{-1} was attained after averaging over 500 scans for all IR spectra reported here.

2.4. Catalytic testing

tert-Butylation of *p*-cresol using *tert*-butanol was carried out under vapor phase conditions in a down flow fixed bed glass reactor using 2 g catalyst. The catalyst was activated at 400 °C

Table 1A
Calculation of the amount of TPA corresponding to a monolayer by surface area data

Sample	S_{BET}	Amount TPA (g)	Amount TPA (mol)	Amount TPA (molecules)	Surface (nm^2)	Surface per TPA
10TT-700	36.9	0.1	3.3E−05	2.0E+19	3.69E+19	1.83
15TT-700	41.2	0.15	5.0E−05	3.0E+19	4.12E+19	1.36
20TT-700	42.2	0.2	6.6E−05	4.0E+19	4.22E+19	1.0
25TT-700	41.3	0.25	8.3E−05	5.0E+19	4.13E+19	0.82
20TT-650	66.8	0.2	6.6E−05	4.0E+19	6.68E+19	1.6
20TT-700	42.2	0.2	6.6E−05	4.0E+19	4.22E+19	1.0
20TT-750	22.1	0.2	6.6E−05	4.0E+19	2.21E+19	0.55
20TT-800	4.2	0.2	6.6E−05	4.0E+19	4.2E+18	0.10

Molecular weight TPA = 3000.

Table 1B
Pyridine adsorption data for the catalyst 20% TPA/TiO_2 700 °C at different activation temperatures

Activation temperature (°C)	B acidity *I* (B)	L acidity I (L)	B/L ratio *I* (B)/I (L)
200	4.7	1.1	4.27
300	0.16	0.03	5.33
400	0.036	0.013	2.7

in a flow of dry air for 5 h followed by cooling to the desired reaction temperature in N_2 atmosphere. Feed containing a mixture of *p*-cresol and *tert*-butanol of desired molar ratio was passed into the reactor with a fixed feed rate (ml h^{-1}) using a syringe pump (Sage instruments model 352) at the desired reaction temperature. The reaction mixture was cooled (ice trap) to room temperature after passing through the catalyst bed and samples were collected at every 1 h interval. They were analyzed on a Shimadzu 14B gas chromatograph, equipped with a flame ionization detector using SE-52 packed column. The identity of the products was confirmed by GC–MS (Shimadzu QP-5000). Conversion and product selectivities calculated from gas chromatographic analysis were expressed in wt.% and used in the interpretation of the results.

3. Results and discussion

3.1. Characterization of the catalysts

3.1.1. Surface area

The pure titanium (IV) hydroxide dried at 120 °C showed a surface area of 247 m^2 g^{-1}; after calcination at 700 °C, the surface area decreased to 6.3 m^2 g^{-1}. Addition of TPA to the support resulted in an increase in surface area and was maximum at 20% TPA loading (Tables 1A and 1B). This is due to the strong interaction of TPA with the support, which reduces the surface diffusion of titania and inhibits sintering and stabilizes the anatase phase of titania, leading to an increase in surface area to higher thermal stability of the catalyst [25–27]. Above 20% TPA loading, surface area did not change appreciably, possibly due to the partial or high fragmentation of TPA units or formation of crystalline WO_3, which likely narrowed or plugged the pores of the samples. The amount of TPA corresponding to a monolayer calculated for all the catalysts is given in Tables 1A and 1B. The monolayer coverage at 700 °C seems to 20% TPA on TiO_2.

3.1.2. X-ray diffraction

The bulk structure of pure TiO_2 and of supported HPA catalysts were determined by powder X-ray diffraction (Fig. 1). For pure titania an amorphous behavior was observed below 350 °C corresponding to and it, consists of a mixture of anatase, brookite and rutile phases. When increasing the calcination temperature, the amount of the anatase phase increased and became predominant [28] at 500 °C. Upon heating at 700 °C the anatase phase of titania ($2\theta = 24.87$ Å) was completely transformed into the rutile phase ($2\theta = 27.20$ Å), as shown in Fig. 1(A).

The XRD patterns of the catalysts with different TPA loadings calcined at 700 °C show the role of TPA which strongly influences the crystallization of titanium hydroxide into titania [29,30] and the development of new textural properties with temperature as compared to pure titania. The catalysts with low TPA loadings calcined at 700 °C, show only the anatase phase this phase becoming dominant for catalysts with 20% TT-700 as shown in Fig. 1(B). This catalyst was amorphous when calcined below 350 °C and as the calcination temperature increased, titania crystallized progressively to anatase phase. At 700 °C, the catalyst existed mainly in the anatase phase ($2\theta = 24.87$), suggesting that the phase transition of anatase to rutile is shifted to higher temperature in presence of TPA. In addition, for up to a 20% TPA loading for catalysts calcined at 700 °C, no diffraction lines attributed to the crystalline TPA or its decomposition products were observed, indicating that TPA has been highly dispersed on the support. When TPA loading exceeded 20%, it did not interact with titania support leading to its decomposition as shown in Fig. 1(B-d). At a calcination temperature above 700 °C for 20% TPA loading decomposition occurs also as shown by the appearance of the characteristic crystalline tungsten oxide (WO_3) phase and is accompanied by the anatase to rutile phase transformation as indicated by the peaks (23 and 24 Å). Effectiveness of the surface species in stabilizing TiO_2 in the anatase phase may be lost at high temperatures, because TiO_2 particles diffuse into the bulk, decompose, and desorb, or "dewet" and agglomerate to form poorly interacting clusters as a separate phase [31]. It can also be pointed out that the anatase to rutile phase transition corresponds to the decrease of the BET surface area.

3.1.3. XPS study

The XPS investigation of binding energies and intensities of the surface elements provides information on the chemical

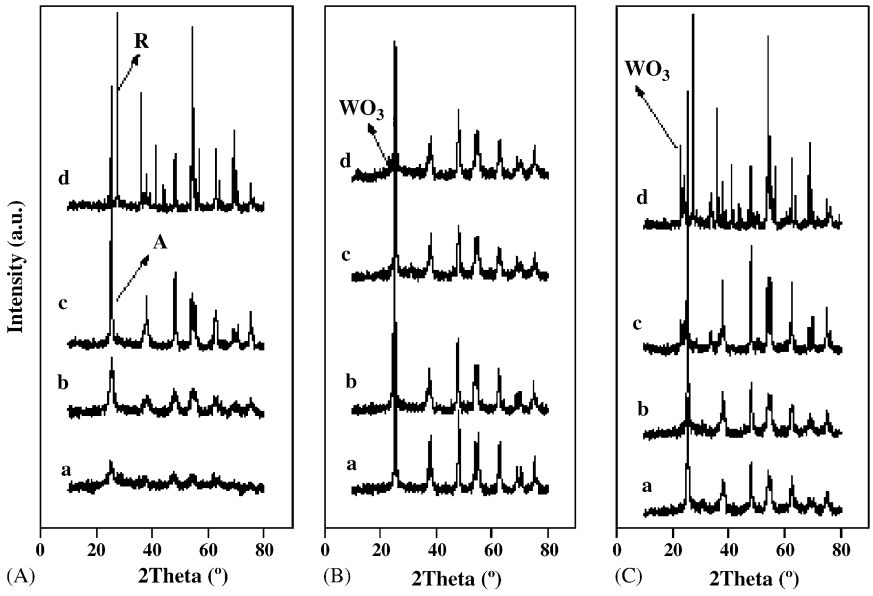

Fig. 1. X-ray diagrams of (A) TiO_2 calcined at (a) 120 °C, (b) 300 °C, (c) 500 °C, (d) 700 °C. (B) The catalyst with different TPA loadings calcined at 700 °C: (a) 10%, (b) 15%, (c) 20%, (d) 25%. (C) Twenty percent TT catalyst calcined at different temperatures (a) 650 °C, (b) 700 °C, (c) 750 °C, (d) 800 °C.

states and relative quantities of the outermost surface compounds. Fig. 2(A) shows the characteristic Ti 2p XPS spectra of the TPA/TiO_2 catalysts after calcination at 700 °C as a function of TPA content. The binding energy of Ti $2p_{3/2}$ orbital is shifting from 458.9 to 458.63 eV (i.e., 0.27) [32]. This might be due to an electron transfer from the terminal oxygen atoms of TPA to the support resulting in a charging of the surface particles, which could promote releasing proton from TPA and increase in Brönsted acidity. Another possibility explaining this pretreatment effect is a modification of the particle–support interaction leading to lower proton releasing energy and resulting in an increase of the Brönsted acidity of the catalyst.

The W 4f XPS spectra of samples with various TPA loadings corresponding to different samples are shown in Fig. 3. The spectra of the catalysts with more than 10 wt.% TPA are quite similar with two peaks at 35.8 and 37.9 eV, in agreement with the literature data [33]. In contrast the spectrum of the 10% TPA/TiO_2 sample is strongly affected by the interaction with the support.

As shown by XRD crystalline WO_3 appears when the TPA loading is higher than the monolayer dispersion capacity (>20%

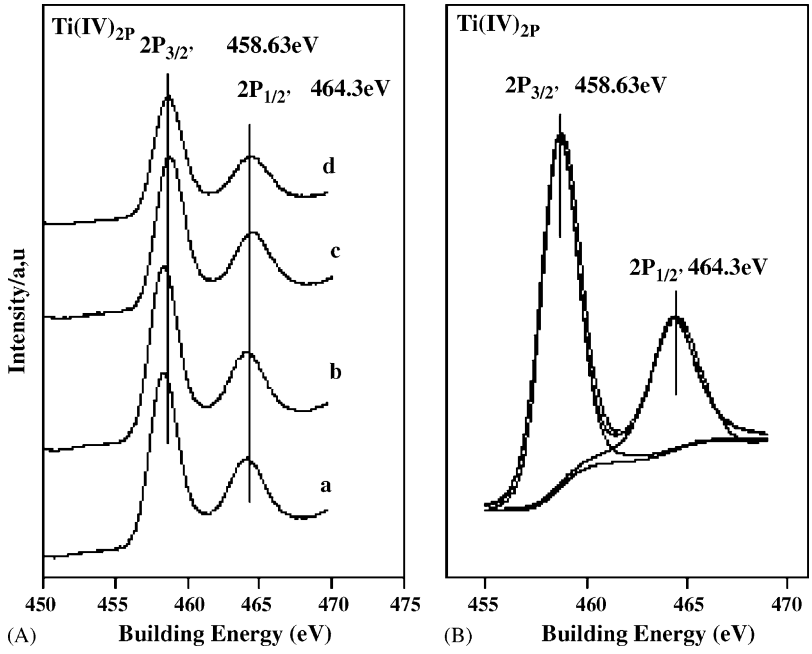

Fig. 2. (A) Ti 2p XPS spectra of TiO_2 with different TPA loadings: (a) 10%, (b) 15%, (c) 20%, (d) 25%. (B) Peak-fitting spectrum of Ti 2p of the (a) 20% TT-700 catalyst.

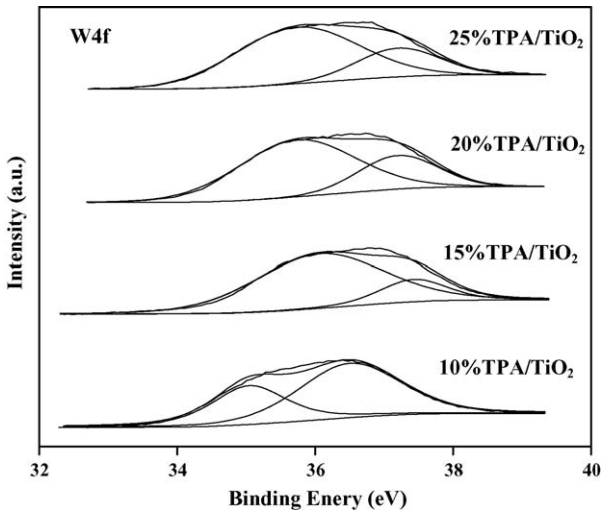

Fig. 3. Peak-fitting XPS spectra of the W 4f region for the catalyst with different TPA/TiO_2 catalysts calcined at 700 °C.

TPA/TiO_2) but has little effect on the phase transformation of the samples. For the supported metal oxide samples, it has been shown that XPS metal-to-support intensity ratios can provide important information regarding the dispersion and crystalline size of the supported metal particles [34–36]. The W 4d peak was used to quantify the amount of tungsten on the support. The correlation between the W 4d/Ti 2p XPS intensity ratios and the loading amount of TPA in the TPA/TiO_2 samples is shown in Fig. 4. Two lines with different slopes can be discerned. For TPA loadings lower than 20% the W 4d/Ti 2p intensity ratio increases relatively linearly while it remains constant for higher loadings. In agreement with the XPS data on the W 4f peak, it can be pointed out that for the 10% TPA/TiO_2 sample this ratio is quite zero, corresponding to the strong interaction with the support.

When the TPA loading is beyond 20% TPA, crystalline WO_3 starts to form. Since for a given amount, the contribution of crystalline WO_3 to $I_{W\ 4d}$ is much smaller than that of highly dispersed TPA, the degree of increase of $I_{W\ 4d}/I_{Ti\ 2p}$ is much smaller once crystalline WO_3 is deposited. The point of intersection of the two lines can be regarded as a threshold corresponding to

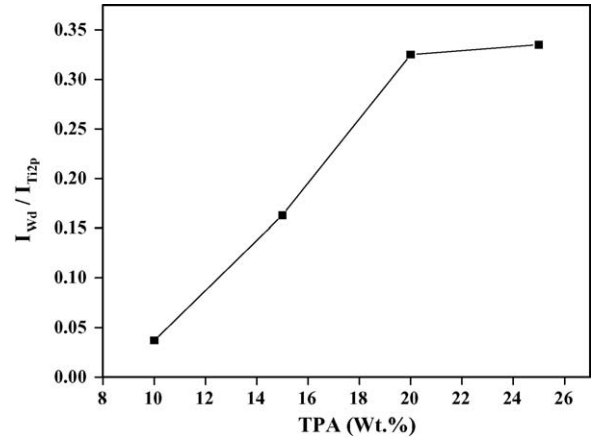

Fig. 4. XPS peak intensity ratio of $I_{W\ 4d}/I_{Ti\ 2p}$ vs. the content of TPA in TPA/TiO_2 samples calcined at 700 °C.

the monolayer dispersion capacity. The monolayer dispersion capacity of the TPA/TiO_2 system calcined at 700 °C is about 20% TPA on TiO_2 (20% TT-700). The above results are consistent with the conclusions obtained from BET surface area and XRD studies that only highly dispersed TPA species exist in the low loading samples whilst an additional crystalline WO_3 phase is formed in samples with TPA loadings higher than the monolayer dispersion capacity (>20% TPA/TiO_2). Furthermore, it can be concluded from XRD and XPS results that the monolayer capacity of TPA on anatase TiO_2 is about 20%.

3.1.4. ^{31}P MAS NMR studies

Fig. 5 shows the ^{31}P MAS-NMR spectra of some of the catalysts, with various loadings (Fig. 5(A)) and for the same loading after various calcination temperatures (Fig. 5(B)). In all cases the spectrum is relatively broad and is composed of numerous components, as seen in Fig. 6 which displays the deconvolution of the spectrum of the 20% TT-700 sample [37,38]. This deconvolution was made on all samples, the results being given in Table 2. The signals near 0 ppm correspond to phosphate species resulting from the decomposition of the Keggin unit while intact TPA will give lines at −13 and −18 ppm depending on its hydration degree. The signal near −9 ppm can be attributed to a lacunary Keggin unit formed upon partial decomposition of TPA on TiO_2. When looking at the data of Fig. 5 and Table 2, the following conclusions can be made:

3.1.4.1. Evolution as a function of temperature. When increasing the temperature the Keggin unit decomposes but after calcination at 650 °C a great amount of intact TPA remains (Fig. 5(B-a)). The transformation of the anatase to rutile phase of TiO_2 observed above is also accompanied by the decomposition of the TPA Keggin compound.

3.1.4.2. Evolution as a function of the TPA loading. When the TPA loading increases, the proportion of intact or lacunary Keggin units increases, while the amount of decomposed polyanion remains quite constant, in terms of moles per gram of support. This fact can be explained easily. When TPA is adsorbed on TiO_2 it goes first on the more basic sites which will decompose it totally. When higher amounts are adsorbed they go on less basic sites where there is only a partial or no decomposition of the Keggin unit. If we look at the data of Table 2, it seems that the decomposition of TPA occurs for loadings of ca. 10%, in agreement with the above results of XPS and BET surface area. As a consequence we can propose that at low loadings TPA is decomposed leading to a stabilization of the TiO_2 support while higher amounts of TPA will give the higher acidity over the stabilized support required for the catalytic reaction.

3.1.5. TPD of NH_3

The ammonia adsorption–desorption technique enables determination of the strength of acid sites present on the catalyst surface together with total acidity. The NH_3-TPD profiles of the catalysts with different TPA loadings and of the 20% TT catalysts calcined at different temperatures are shown in Fig. 7

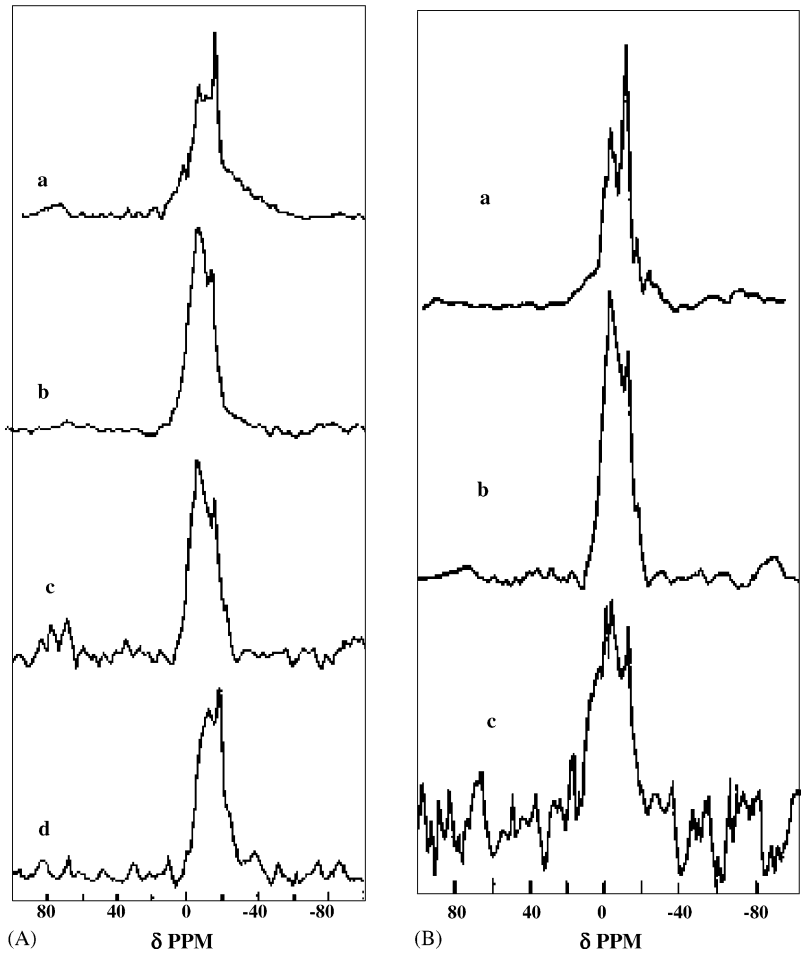

Fig. 5. ^{31}P MAS NMR spectra of (A) catalysts with different TPA loading: (a) 10%, (b) 15%, (c) 20%, and (d) 25% TT calcined at 700 °C and (B) 20% TT catalyst calcined at temperature (a) 650 °C, (b) 700 °C, and (c) 750 °C.

while the amounts of NH_3 desorbed per nm^2 are presented in Tables 1A and 1B.

All samples showed a broad TPD profile, however, the acidity values increase and the shift of desorption of ammonia to higher temperature reveal that the acidity increases as the TPA loading increases and surface acid strength was more in 20% TT-700 as compared to other loadings. It is evident from Tables 1A and 1B

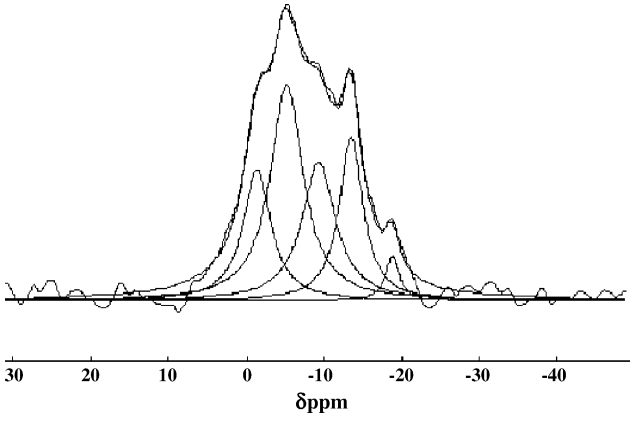

Fig. 6. Deconvolutions of ^{31}P NMR spectrum of 20% TT catalyst calcined at 700 °C.

Table 2
^{31}P NMR peak position and intensity data from the deconvolutions

Catalyst	Peak position (δ ppm)	Normalized integral intensity
10% TPA/TiO_2	4	2
	1	1
	−4	17
	−9	15
	−12	54
	−13	11
15% TPA/TiO_2	−1	15
	−6	57
	−13	27
	−17	1
20% TPA/TiO_2	−1	18
	−5	35
	−9	23
	−13	20
	−18	4
25% TPA/TiO_2	−4	1
	−7	2
	−9	5
	−13	44
	−17	43
	−24	5

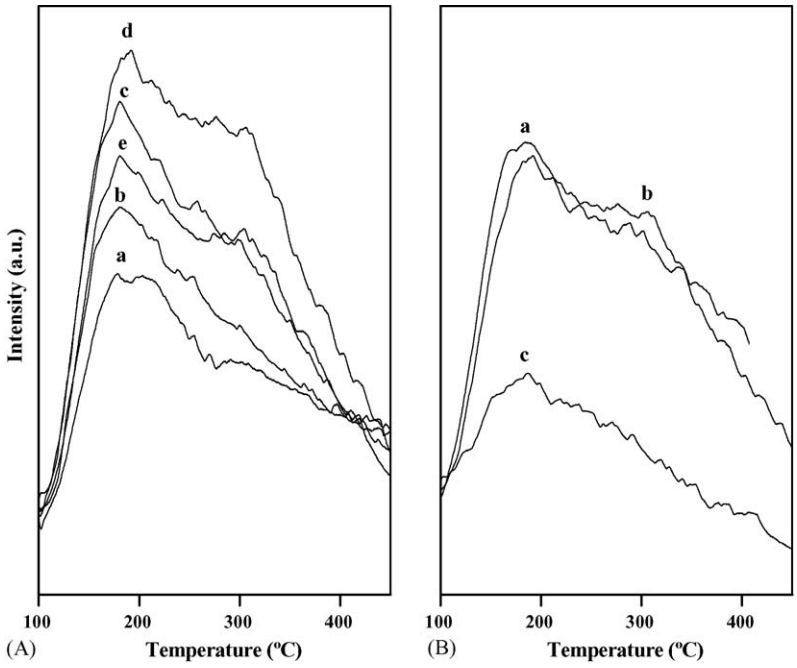

Fig. 7. NH_3-TPD profile of (A) catalyst with different TPA loadings calcined at 700 °C: (a) 0%, (b) 10%, (c) 15%, (d) 20%, (e) 25% and (B) 20% TT catalyst calcined at temperatures: (a) 650 °C, (b) 700 °C, (c) 750 °C .

that there was an initial increase in the acidity until 20% loading, after which it decreased with further loading. It can be concluded that for low TPA loading (∼10%), surface of the titania is not covered completely by TPA which is also at least partially decomposed. However, at 20% TPA loading a complete monolayer active phase was formed, which is also observed by ratio of XPS peak area of the W d and Ti 2p orbital Fig. 4; at higher loading (i.e., >20 wt.% TPA), it decomposes at least partially into its polyoxometales as confirmed by XRD data. The highest acidity corresponds to monolayer coverage of TPA (i.e., 20 wt.% TT calcined at 700 °C), where charge transfer from surface terminal double bonded oxygen to support leads to lower the proton releasing energy from the active species due to the strong interaction of TPA and titania supported (supported by ^{31}P CPMAS NMR and XPS data). Tables 1A and 1B indicates that the total acidity increases up to 700 °C and the acidic strength is more. Further increases in calcination temperature above 700 °C leads to decreasing acidity and also catalytic activity, which is due to complete decomposition of TPA into WO_3 crystallites.

3.1.6. FTIR pyridine adsorption

Adsorption of pyridine as a base on the surface of solid acids is one of the most frequently applied methods for the characterization of surface acidity. The use of IR spectroscopy to detect adsorbed pyridine allows one to distinguish among different acid sites. The FTIR pyridine adsorption spectra of catalysts with different TPA loadings calcined at 700 °C and 20% TT catalysts calcined at different temperatures are shown in Fig. 8. The spectra showed sharp pyridine absorption bands at 1489, 1446, 1636, and 1542 cm^{-1}. Pyridine molecules bonded to Lewis acid sites absorbed at 1446 cm^{-1}, whereas those responsible for Brönsted acid sites (pyridinium) showed absorbance at 1542 and 1636 cm^{-1} [39]. The band at 1489 cm^{-1} is a combined band originating from pyridine bonded to both Brönsted and Lewis

Table 3
Surface areas, NH_3-TPD and pyridine adsorption of all the catalysts

Catalyst	Surface area (m^2 g^{-1})	Acidity[a] (NH_3, nm^{-2})	B acidity[b] *I* (B)	L acidity[b] *I* (L)	B/L ratio[b] *I* (B)/*I* (L)
T-700	6.3	ne[c]	ne[c]	ne[c]	ne[c]
10TT-700	36.9	2.36	3.6	2.89	1.24
15TT-700	41.2	2.86	5.68	1.8	3.15
20TT-700	42.2	3.42	4.7	1.1	4.27
25TT-700	41.3	2.6	3.29	2.49	3.15
20TT-650	66.8	ne[c]	7.58	3.49	2.05
20TT-750	22.1	1.25	0.87	0.48	1.81
20TT-800	4.2	ne[c]	ne[c]	ne[c]	ne[c]

[a] Acidity values obtained from NH_3-TPD.
[b] For catalysts with different TPA loading, calcined at 700 °C, pyridine adsorption was carried out under vacuum and for 20% TT catalyst with different calcination temperature, it was carried out under N_2 flow.
[c] Not evaluated.

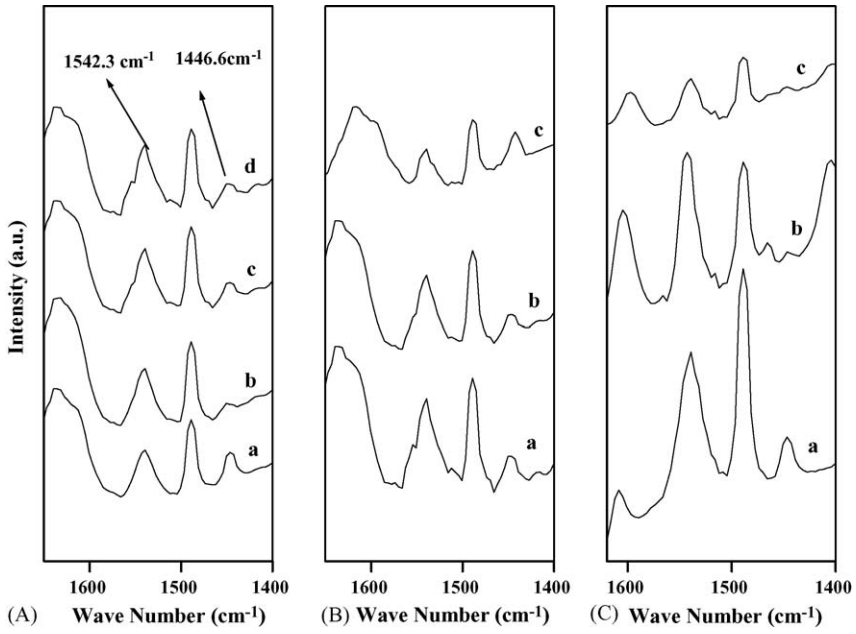

Fig. 8. FTIR pyridine adsorption spectra of (A) catalyst with different TPA loading calcined at 700 °C: (a) 10%, (b) 15%, (c) 20%, (d) 25%; (B) 20% TT calcined at temperatures: (a) 650 °C, (b) 700 °C, (c) 750 °C after in situ activation at 200 °C and (C) 20% catalyst at different in situ activation temperature (a) 200 °C, (b) 300 °C, (c) 400 °C.

acid sites. The intensity of Brönsted (B) and Lewis (L) acid sites, obtained from the absorbance at 1542 and 1446 cm^{-1} [40], and the corresponding B/L intensity ratios calculated and are shown in Table 3. At low loading, the catalyst showed both Brönsted acidity and Lewis acidity; with an increase in loading Lewis acidity decreased, whereas Brönsted acidity increased and reached a maximum at 20% TPA loading. An increase in TPA loading above 20% decreased the Brönsted acidity, but with Lewis acidity remaining similar to that of 20% catalyst. The decrease in acidity above 20% could be due to the formation of crystalline WO_3, which prevents the accessibility of pyridine to the active sites. As in the case of catalysts with different loadings, the nature of acidity also depends on calcination temperature. At low calcination temperature (<650 °C), the catalyst 20% TT showed both Brönsted acidity and Lewis acidity; by increasing calcination temperature the Brönsted acidity increased up to 700 °C and was predominant at this calcination temperature. Moreover, the catalyst 20% TT-700 showed higher Brönsted acidity, under all activation temperatures (B/L intensity ratio) of the catalyst. These results clearly show that at lower loading, the catalyst showed mainly Lewis acidity and this could be due coordinately unsaturated Ti^{4+} species on the surface. An increase in TPA loading above 20% decreased the Brönsted with both loading and calcination temperature up to a monolayer TPA on TiO_2 this could be due to interaction between support and active sites that leads to charge delocalization from terminal double bonded oxygen of TPA to titania and leads to ease in releasing protons and 20% TT calcined above 700 °C showed decrease in Brönsted acidity due to the formation of crystalline WO_3 and monophosphate phase, which is also supported from XRD results.

3.2. Catalytic activity

tert-Butylation of *p*-cresol by *tert*-butanol catalyzed by 20% TT-700 gave mainly 2-TBC, 2,6-DTBC and CTBE as products as shown in Scheme 1. This reaction is an example of electrophilic substitution of *tert*-butyl cation formed by *tert*-butanol on the aromatic ring to give C-alkylated products and also small amounts of O-alkylated product. The substitution at meta position with respect to –OH group in *p*-cresol has not been favored due to the steric hindrance of methyl and *tert*-butyl groups. O-alkylation resulted in the formation of ether was also least favored with the above catalyst under vapor phase conditions.

To study the effect of TPA loading on TiO_2 in alkylation of *p*-cresol with *tert*-butanol, the catalysts with different TPA loading (10–25 wt.%) on TiO_2 were prepared and calcined at 700 °C.

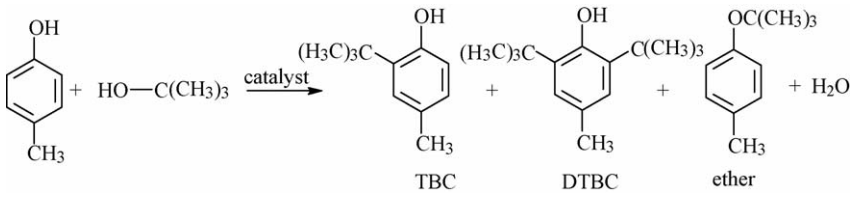

Scheme 1.

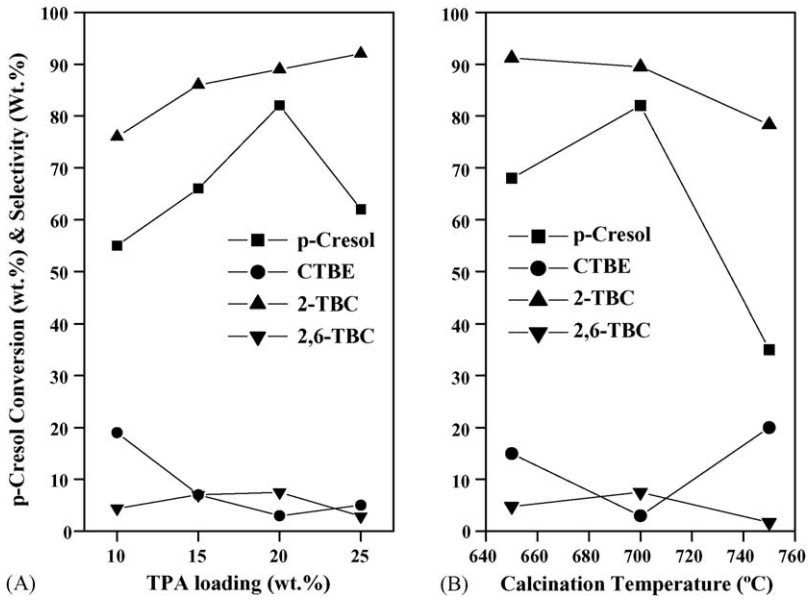

Fig. 9. (A) Effect of different TPA loading (wt.%) on TiO_2. Conditions: catalyst calcination = 700 °C; temperature = 130 °C; feed = 10 ml h^{-1}; Bu/Cr molar ratio = 3; time = 3 h. (B) Effect of calcination temperature. Conditions: catalyst = 20% TT-700; temperature = 130 °C; feed = 10 ml h^{-1}; Bu/Cr molar ratio = 3, time = 3 h.

The reaction was carried out at 130 °C, feed 10 ml h^{-1} of *tert*-butanol to *p*-cresol (Bu/Cr) molar ratio 3. Fig. 9(A) shows the effect of TPA loading on the conversion of *p*-cresol and the product selectivities. Catalyst with 20% TT-700 loading was found to be the most active and gave 2-TBC (89.5%), 2,6-DTBC (7.5%) and CTBE (3%) at conversion of *p*-cresol (82%). These observations are in concurrence with the catalyst characterization, which indicated that 20% TPA loaded catalyst has the highest acidity (Fig. 7) and hence most active in the butylation of *p*-cresol by *tert*-butanol. Interestingly, 10 and 25% TPA loaded catalysts under the above reaction conditions gave less conversion of *p*-cresol but more of ether. This indicated that the catalysts having less acidity favored O-alkylation to form ether.

The effect of calcination temperature on 20% TT catalyst calcined from 650 to 750 °C is used to study the change in catalytic activity with calcination temperature. It is seen from Fig. 9(B) that the calcination temperature has a profound effect on catalytic activity. The catalyst calcined at 650 °C gave 67% *p*-cresol conversion, which increases to 82% at 700 °C. Further increase in calcination temperature decreases *p*-cresol conversion and selectivity to different alkylated products as shown in Fig. 9(B). A decrease in CTBE selectivity results in an increase in 2-TBC selectivity from 80.2 to 90%. As the calcination temperature increased from 700 to 750 °C, the selectivity to CTBE increased from 12.1 to 53%, while the selectivity to 2-TBC decreased from 85.7 to 47%.

The effect of reaction temperature was carried out using 20% TT-700 at different temperatures in the range 110–170 °C maintaining constant conditions as, feed rate 10 ml h^{-1} of Bu/Cr mole ratio 2. The conversion of *p*-cresol was maximum at 130 °C (Fig. 10(A)) with maximum selectivity to 2-TBC. Ether was formed considerably (22%) at 110 °C, indicated that lower temperature favored ether formation. Also, at higher temperatures (>130 °C), dealkylation of 2,6-DTBC to 2-TBC occurred, which slightly increased the selectivity for 2-TBC. Considering the above observations 130 °C was chosen as the suitable temperature for further study.

To study the influence of *tert*-butanol/cresol mole ratio in the range 1–4, experiments were carried at 130 °C and feed 10 ml h^{-1} using 20% TT-700. The conversion of *p*-cresol was increased up to Bu/Cr mole ratio 3 and then decreased with further increase. However, selectivities for C- and O-alkylated products remained almost the same (Fig. 10(B)) with higher selectivities for 2-TBC. The conversion of *p*-cresol was low at lower molar ratios, which could be due to the preferential adsorption of *p*-cresol (*p*-cresol is more polar than *tert*-butanol) on the catalyst surface reducing the adsorption of *tert*-butanol over the catalyst surface. Hence, higher *tert*-butanol concentration favored (Bu/Cr molar ratio 3) higher conversion of *p*-cresol. However, the conversion of *p*-cresol decreased at Bu/Cr molar ratio 4, which could be due to the parallel reaction of *tert*-butanol leading to the formation of its side products (dehydration of *tert*-butanol to isobutylene) and decreasing its availability for the main reaction.

The effect of feed (ml h^{-1}) on *tert*-butylation of *p*-cresol was carried out at different feed ranging from 10 to 20 ml h^{-1} at 130 °C and Bu/Cr molar ratio of 3 and the results are shown in Fig. 11(A). Conversion of *p*-cresol decreased with increase in feed (ml h^{-1}) due to shorter contact time at higher space velocities (express every thing in WHSV to use the term space velocity). The selectivity for 2-TBC remained almost unchanged. However, selectivity for 2,6-DTBC was found to be more at lower feed (10 ml h^{-1}) and decreased with further increase. The longer contact time favored 2,6-DTBC formation (9.4%), while shorter contact time facilitated ether formation (7.2%).

The activity of the 20% TT-700 catalyst was studied as a function of time in the butylation of *p*-cresol at 130 °C, feed 10 ml h^{-1} and Bu/Cr molar ratio of 3 and the results are shown in Fig. 11(B). The reaction was carried out for 10 h and conversion of *p*-cresol decreased from 82 to 70% in the course of 6 h and

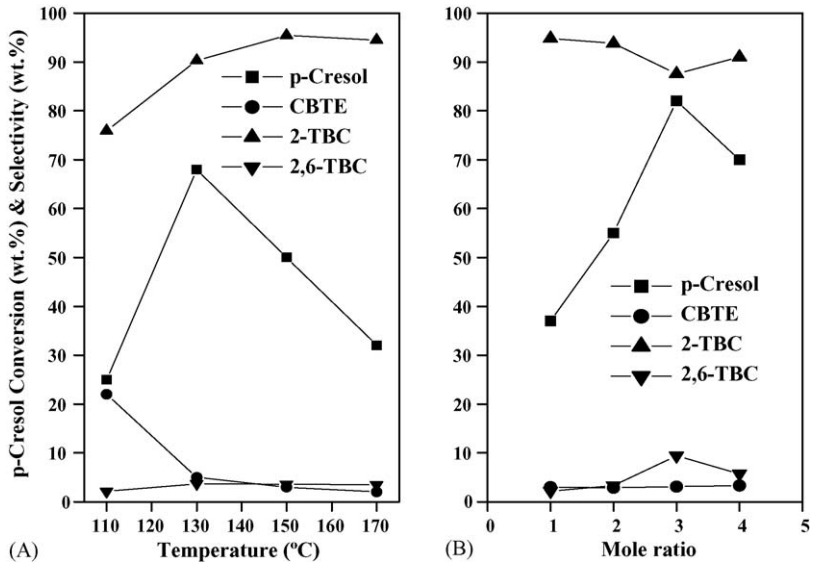

Fig. 10. (A) Effect of reaction temperature. Conditions: catalyst = 20% TT-700; flow rate = 10 ml h^{-1}; Bu/Cr molar ratio = 2, time = 3h. (B) Effect of *tert*-butanol to *p*-cresol molar ratio. Conditions: catalyst = 20% TT-700; temperature = 130 °C; feed = 10 ml h^{-1}; time = 3 h.

then remained constant. The selectivity for 2-TBC increased while that of 2,6-DTBC decreased up to 5 h and then attained steady state.

For catalyst regeneration, the used catalyst after each reaction was regenerated by calcination at 400 °C for 5 h and used for all the experiments. We observed that the regenerated catalyst gave almost the same results as that of the fresh catalyst with respect to conversion of *p*-cresol and product selectivities. This demonstrates the catalyst's regenerability and reuse in industrial applications for alkylation reactions.

3.3. Activity comparison with zeolites, WO_3/ZrO_2 and montmorillonite K-10

The alkylation of *p*-cresol with *tert*-butanol was studied using sulfated zirconia (SZ), WO_3/ZrO_2, zeolites like USY, H-β and montmorillonite K-10 (Fig. 12). The 20% TT-700 catalyst was found to be the most active catalyst for this reaction. Except SZ, WO_3/ZrO_2, the *p*-cresol conversion of other catalysts is less than 25% under the reaction conditions, which may be due to the difference in pore structure and acidity.

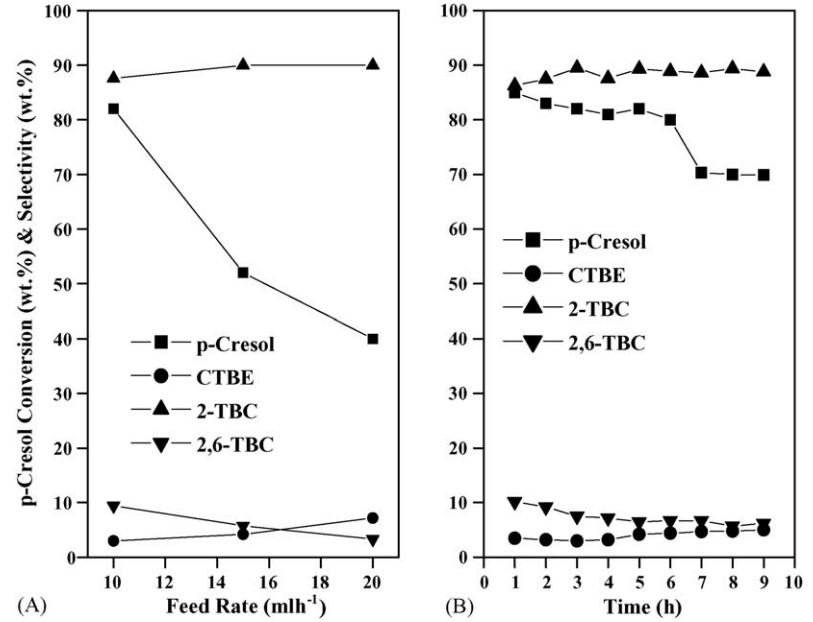

Fig. 11. (A) Effect of feed. Conditions: catalyst = 20% TT-700; temperature = 130 °C; Bu/Cr molar ratio = 3; time = 3 h. (B) Study of time on stream. Conditions: catalyst = 20% TT-700; temperature = 130 °C; Bu/Cr molar ratio = 3; feed = 10 ml h^{-1}.

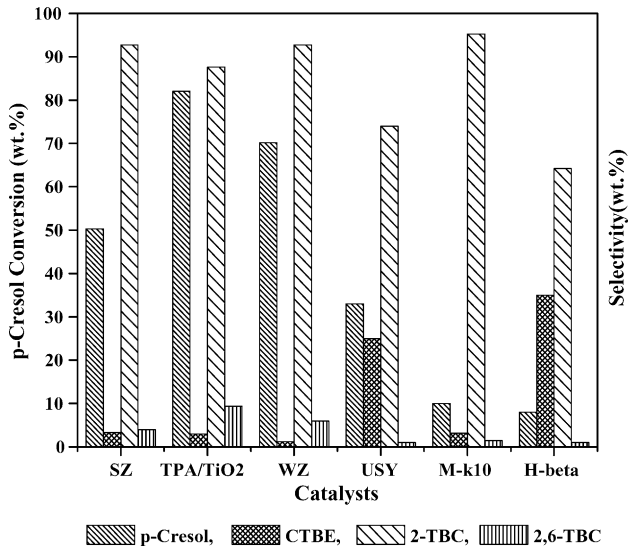

Fig. 12. Comparison of catalysts. Conditions: catalysts = SZ, WO_3/ZrO_2, USY, K-10 mont, H-β and TPA/TiO_2 (20% TT-700); temperature = 130 °C; Bu/Cr molar ratio = 3; feed = 10 ml h^{-1}.

4. Conclusions

The results presented in this work provided a detailed description of the changes in the acidic features of series of TPA modified titania, which was tested in the vapor phase alkylation of *p*-cresol with *tert*-butanol in a continuous fixed bed down flow reactor. The catalytic activity mainly depended on TPA coverage and highest activity corresponded to monolayer coverage of TPA on titania and the amount of TPA in Keggin calculated from ^{31}P MAS NMR Dim fit software. The catalytic activity was compared with sulfated zirconia, zeolites like USY, H-β and montmorillonite K-10 under the optimized identical reaction conditions. The catalytic activity of sulfated zirconia was found to be lower than that of 20% TT-700 and hence the heteropoly acid modified titania catalysts provides an alternate to other similar catalysts for acid catalyzed reactions.

Acknowledgements

This work was financially supported by DST New Delhi under SERC funding. GV Shanbhag is thankful to CSIR for awarding the senior research fellowship.

References

[1] M. Misono, T. Okuhara, Chemtech 23 (11) (1993) 23.
[2] J.M. Thomas, Sci. Am. 112 (1992) 2664.
[3] J. Pospisil, Poly. Deg. Stab. 20 (1988) 181.
[4] J. Murphy, The Additives for Plastics Handbook, Elsevier Advanced Technology, Oxford, 1996.
[5] R.C. Huston, W.C. Lewis, J. Am. Chem. Soc. 53 (1931) 2379.
[6] H. Hart, E.A. Haglund, J. Org. Chem. 15 (1956) 396.
[7] E. Santacesaria, R. Silvani, P. Wilkinson, S. Carra, Ind. Eng. Chem. Res. 27 (1988) 541.
[8] Widdecke, Hartmut, Chem. Ing. Tech. 52 (1980) 825.
[9] G.D. Yadav, T.S. Thorat, Ind. Eng. Chem. Res. 35 (1996) 721.
[10] Z.X. Su, T.J. Wang, React. Funct. Polym. 28 (1995) 97.
[11] J. Zhang, Z. Zhu, C. Li, L. Wen, E. Min, J. Mol. Catal. A 198 (2003) 359.
[12] J. Kaur, K. Griffin, B. Harrison, V. Kozhevnicov, J. Catal. 208 (2002) 448.
[13] E.L. Salinas, J.G.H. Cortez, I. Schifter, E.T. Garcia, J. Novarrete, A.G. Carrillo, T. Lopez, P.P. Lottici, D. Bersani, Appl. Catal. A 193 (2000) 215.
[14] A. Molnar, C. Keresszegi, B. Torok, Appl. Catal. A 189 (1999) 217.
[15] C. Hu, Y. Zhang, L. Xu, G. Peng, Appl. Catal. A 177 (1999) 237.
[16] G.D. Yadav, N.S. Asthana, V.S. Kamble, J. Catal. 217 (2003) 88.
[17] A. Molnar, T. Beregszaszi, A. Fudala, P. Lentz, J. Nagy, Z. Konya, I. Kiricsi, J. Catal. 202 (2001) 379.
[18] Y. Izumi, M. Ogawa, K. Urabe, Appl. Catal. A 132 (1995) 127.
[19] B.M. Devassy, S.B. Halligudi, S.G. Hegde, A.B. Halageri, F. Lefebvre, Chem. Commun. (2002) 1074.
[20] S. Sarish, B.M. Devassy, S.B. Halligudi, J. Mol. Catal. A 235 (2005) 44.
[21] B.M. Devassy, G.V. Shanbhag, F. Lefebvre, S.B. Halligudi, J. Mol. Catal. A 210 (2004) 125.
[22] C.N. Satterfield, Heterogeneous Catalysis in Industrial Practice, 2nd ed., McGraw-Hill, New York, 1991, p. 123.
[23] M. del Arco, A. Caballero, P. Malet, V. Rives, J. Catal. 113 (1988) 120.
[24] M. Gopal, W.J. Moberlychan, L.C. De Jonghe, J. Mater. Sci. 32 (1997) 6001.
[25] S. Eibil, B.C. Gates, H. Knozinger, Langmuir 17 (2001) 107.
[26] X.-F. Yu, N.-Z. Wu, H.-Z. Huang, Y.-C. Xie, Y.-Q. Tang, J. Mater. Chem. 11 (2001) 3337.
[27] J.R. Sohn, J.S. Han, Appl. Catal. A: Gen. 298 (2006) 168.
[28] J.R. Sohn, W.C. Park, Bull. Korean Chem. Soc. 22 (12) (2001) 1303.
[29] E. Ortiz-Islas, T. Lopez, R. Gomez, M. Picquart, D.H. Aguilar, P. Quintana, Appl. Surf. Sci. 252 (2005) 853.
[30] S. Eibl, B.C. Gates, H. Knoziger, Langmuir 17 (2001) 107.
[31] D.G. Barton, S.L. Soled, G.D. Meitzner, G.A. Fuentes, E. Iglesia, J. Catal. 181 (1999) 57.
[32] X.-L. Yang, W.-L. Dai, C. Guo, H. Chen, Y. Cao, H. Li, H. He, K. Fan, J. Catal. 234 (2005) 438.
[33] P.A. Jalil, M. Faiz, N. Tabet, N.M. Hamdan, Z. Husssain, J. Catal. 217 (2003) 292.
[34] F.P. Kerkhof, J.M. Moulijn, J. Phys. Chem. 83 (1979) 1612.
[35] U. Balachandran, N.G. Eror, J. Solid State Chem. 42 (1982) 276.
[36] X.-F. Yu, N.-Z. Wu, H.-Z. Huang, Y.-C. Xie, Y.-Q. Tang, J. Mater. Chem. 11 (2001) 3337.
[37] J.C. Edwards, C.Y. Thiel, B. Brian, J.F. Knifton, Catal. Lett. 51 (1998) 77.
[38] E.C. Decano, J.C. Edwards, T.R. Scalzo, D.S. Strorm, J.W. Bruno, J. Catal. 132 (1993) 657.
[39] G. Busca, Catal. Today 41 (1998) 191.
[40] B.H. Davis, R.A. Keogh, S. Alerasool, D.J. Zalewski, D.E. Day, P.K. Doolin, J. Catal. 183 (1999) 45.